Geochemistry and Microstructure Characterization of Kerogen in Chinese Cambrian Shale: A Combined Experimental and Molecular Simulation Study*

Liang Huang[1,2], Zhengfu Ning[1], Ke Wang[1], Qing Wang[1], Zheng Sun[1], and Fengrui Sun[1]

Search and Discovery Article #70363 (2018)**
Posted October 8, 2018

*Adapted from extended abstract based on poster presentation given at AAPG 2018 Annual Convention & Exhibition, Salt Lake City, Utah, United States, May 20-23, 2018
 DOI:10.1306/70363Huang2018

[1]State Key Laboratory of Petroleum Resources and Prospecting, China University of Petroleum (Beijing), Beijing, China (nzf@cup.edu.cn)
[2]Department of Chemical and Biomolecular Engineering, University of California, Berkeley, Berkeley, CA, United States

Abstract

In this work, a combination of solid-state ^{13}C nuclear magnetic resonance (^{13}C NMR) spectroscopy and X-ray photoelectron spectroscopy (XPS) were adopted to characterize the chemical structure of kerogen in Chinese Cambrian shale. These direct characterization results were utilized to develop an averaged molecular structure of Cambrian kerogen. A representative molecular model of Cambrian kerogen was constructed using molecular simulation method. Microstructure properties of the kerogen model were further investigated. Reasonable consistencies are observed on structural parameters, physical density and porosity between simulated results and experimental data, which validates our kerogen model. Pore volume distribution of the kerogen model shows a monopeak type, with the pore width corresponding to the peak site at ~1.6 Å. In addition to accessible micropores, the kerogen model contains a large amount of inaccessible ultra-micropores, which contribute a lot to the high porosity and specific surface area. Although porous network of the kerogen model is highly connected with few dead pores, throats in this system are mainly inaccessible ultra-micropores. This generated kerogen model can serve as a starting point to study gas storage and transport mechanism in shale organic pores at nanoscale.

Introduction

Shale gas has demonstrated huge potential to relax the increasing fossil energy problem and change the global energy structure due to its abundant reserves. Shale gas is mainly stored in organic nanopores in the form of adsorbed gas, free gas and absorbed gas (Wu et. al., 2016). Adsorbed gas takes up a large proportion of shale gas, which can account for 60-85 % in Lewis Shale (Curtis, 2002). Kerogen is the main contributor to specific surface area and adsorption capacity of shale (Huang et. al., 2017a). A good understanding of gas adsorption behavior in kerogen can facilitate shale gas reserves evaluation, as well as shale gas exploitation (Huang et. al., 2018a).

Experimental measurement and molecular simulation are common techniques for studying gas adsorption behavior in kerogen. Constrained by experimental apparatus, laboratory isothermal measurement cannot be performed at high temperature and pressure conditions. In addition, it is

difficult to gain insights into gas microbehaviors and adsorption mechanisms with experimental method. By contrary, molecular simulation can effectively compensate these limitations of experimental measurement. Construction of reasonable molecular model of kerogen is the prerequisite to studying kerogen adsorption properties at molecular scale (Huang et. al., 2018b, Huang et. al., 2017b).

Laboratory experiments serve as fundamental approaches to characterize structural parameters of kerogen. To date, various experimental methods including chemical approaches and physical approaches have been proposed. Chemical approaches require the decomposition of experimental sample, which may damage some important structural information and bring large uncertainty. Compared with destructive chemical approaches, direct physical characterization experiments can provide more preserving structural information and less associated uncertainties (Kelemen et. al., 2007). Thus, it is widely used for chemical structure characterization. Cambrian marine shale in Sichuan Basin is one of the most important target zones for shale gas exploration and exploitation in China. However, to our best knowledge, there is no reported research on construction of representative molecular model of Cambrian kerogen, and our work aims to fill in this research gap.

In this work, kerogen in Chinese Cambrian shale is targeted. Direct characterization techniques are first adopted to capture its analytical structural parameters. ^{13}C NMR spectroscopy is utilized to characterize the structural information of kerogen skeleton, while XPS is performed to specify the heteroatom groups. An averaged kerogen unit is built based on these analytical data. Thereafter, a representative kerogen model is generated with molecular simulation method. In addition, porous network characterization on this kerogen model is further performed. The realistic kerogen model is expected to serve as a starting point for further theoretical investigations on gas adsorption and transport mechanism in Cambrian kerogen at microscopic scale.

Sample and Methodology

Sample preparation

The investigated shale sample is a black outcrop collected from the Lower Cambrian Niuititang Formation in Sichuan Basin, Southwest China. Large chunks of the sample were crushed first, and then grounded into powders smaller than 75 μm. Thereafter, Soxhlet extraction with toluene was adopted to extract soluble bitumen components. Acid treatments were further performed to isolate kerogen sample from the shale remain. Carbonates were removed by 20 wt% HCl acid, while silicates were removed by a mixture of HCl and HF acids (20 wt% HCl + 40 wt% HF).

Characterization experiments

The kerogen sample was treated by a Thermo Scientific FLASH 2000 CHNS-O Analyzer for elemental analysis. The ^{13}C NMR spectrum was measured at 100.64 MHz by a Bruker AVANCEIII TM-600 MHz spectrometer with the MAS magic angle spinning and using a ZrO_2 rotor (4 mm diameter). A recycle delay time of 3 s and a contact time of 4 ms were adopted in the cross-polarization process. The XPS measurement on kerogen powders was conducted on a Thermo Scientific ESCALAB 250Xi spectrometer using monochromatic Al K_α radiation (1486.6 ev). The sputtering rate was 4 nm/min, and the transmit current was 10 mA.

Modelling methodology

Construction of kerogen structure

Characterization results from elemental analysis, ^{13}C NMR spectrum and XPS measurement were utilized to generate the kerogen structure, following the process below (Huang et. al., 2017a).

1. Data of functional groups and elemental compositions were gathered based on experimental results.
2. A total number of carbon atoms were selected, and the quantity of aromatic carbon was determined according to the obtained aromaticity from experiments.
3. The quantities of H, O, N and S atoms were determined by matching the functional data and elemental compositions.
4. The number of aromatic units was determined to match the experimental result of aromatic carbons per aromatic unit.
5. The initial version of the kerogen structure was generated by connecting the determined units and adjusting the bond lengths, bond angles and dihedral angles.
6. The kerogen structure was refined to match the experimental data of functional groups and elemental compositions.

Structure relaxation

In this work, we adopted geometry optimization and molecular dynamics simulation to build our bulk kerogen model. The relaxation process can refer to our previous work (Huang et. al., 2017a, 2017b, 2018a, 2018b). The Cambrian kerogen unit was first geometry optimized by the smart minimization algorithm to obtain its configuration with local energy minimum. Thereafter, optimized kerogen units were enclosed in a simulation cell, and then relaxed by a succession of molecular dynamics simulations to obtain the configuration of Cambrian kerogen model with global lowest energy.

Pore structure characterization

Probe insertion method was utilized to compute free pore volumes and specific surface areas of Cambrian kerogen model. Randomly inserted probes with fixed Connolly radius roll over the atomic van der Waals surfaces in the kerogen system to determine the solid skeleton surfaces, and the regions wrapped by the skeleton surfaces are identified as free pore volumes (Connolly, 1983). Similarly, a series of spherical probes with stepwise increasing Connolly radius are adopted to detect the corresponding free pore volumes and specific surface areas. Accordingly, the pore volume distribution or specific surface area distribution of Cambrian kerogen model can be computed by differentiating the free pore volumes or specific surface areas with respect to different probe diameters.

Results and Discussion

Chemical structure characterization

^{13}C NMR Spectroscopy

The carbon skeleton structure of Cambrian kerogen was characterized by the ^{13}C NMR spectroscopy (Figure 1a). The kerogen spectrum consists of aliphatic carbon region (0-90 ppm), aromatic carbon region (90-165 ppm) and carbonyl carbon region (165-220 ppm). Compared with the aliphatic carbon region and carbonyl carbon region, the aromatic carbon region has the remarkably largest peak area. Therefore, aromatic carbon is the major carbon type of Cambrian kerogen, while aliphatic carbon and carbonyl carbon mainly serve as linkages or short side chains.

The carbon groups of Cambrian kerogen were quantitatively specified by performing Lorentz peak fitting on the ^{13}C NMR spectrum (Figure 1b). The structural parameters, chemical shifts and fitting areas are listed in Table 1. These structural parameters are utilized to calculate some previously defined lattice parameters (Kelemen et. al., 2007), and the results are shown in Table 2. The aromaticity of Cambrian kerogen is up to 62.95 %, which indicates that aromatic carbons constitute the main structure skeleton of Cambrian kerogen. The aromatic cluster size is proportional to the degree of condensation (X_{BP}). The derived X_{BP} at 0.16 is smaller than that of naphthalene (0.25), indicating that the aromatic cluster for Cambrian kerogen can be represented by 1-2 benzene rings. The derived aromatic substitution (δ=0.53) suggests that 3-4 carbons in each aromatic ring are substituted. In addition to aromatic carbons, the kerogen structure also contains some aliphatic carbons. The aliphatic chain length is calculated as 0.07, indicating that short-branched chains are the major forms of aliphatic carbons. The lattice parameter for aliphatic branch (BI) is 0.53, suggesting that the aliphatic carbons are highly branched for Cambrian kerogen. Moreover, we can also observe some carboxyl or carbonyl groups in the kerogen structure, which can serve as branched side chains or short linkages between aromatic clusters.

XPS results

In this section, the XPS spectrum for Cambrian kerogen (Figure 2a) was analyzed to quantify the elementary forms of heteroatoms. In addition to C, O, N and S, Cambrian kerogen also contains a small trace of Cl and Fe. The observed Cl derives from the remains of acid treatment, while Fe is the main component of pyrite, which cannot be removed by HCl and HF acids. However, since the peak area concentrations for both Cl and Fe are lower than 0.2 %, their effect on the chemical structure of Cambrian kerogen is trivial. Accordingly, we mainly focus on the heteroatoms including O, N and S in Cambrian kerogen.

The elementary forms for heteroatoms were quantitatively specified by conducting peak fitting on the XPS spectrum (Figure 2b-d). The derived results for elementary forms of heteroatoms are shown in Table 3. The C 1s signal on the spectrum was fitted to quantify the elemental forms of O associated with C atom. Ether or alcohol groups are observed to be the main oxygen-containing groups in the kerogen structure. In addition, the kerogen structure contains some carbonyl and carboxyl groups. The fitted results on N 1s signal indicate that amine groups are the dominant nitrogen-containing groups in the kerogen structure. Besides, the Cambrian kerogen contains a small amount of stable pyridine and

pyrrole groups. The nitrogen oxide groups from the acid treatment are observed to be well removed. The fitted results on S 2p signal indicate that S mainly exists in the organic components, and sulfoxide group is the dominant sulfur-containing group, with its area ratio being up to 86.43 %, followed by the thiophene group at 13.57%.

Molecular structure of Cambrian kerogen

Following the construction process the "Construction of Kerogen Structure" section, the representative Cambrian kerogen structure (Figure 3) is generated, with its compositions and structural parameters listed in Table 4. The atomic compositions of Cambrian kerogen are consistent with the elemental analysis results. The structure skeleton is composed of nine naphthalenes and six benzenes linked by branched aliphatic carbons and heteroatom groups. The lattice parameters such as degree of condensation, aliphatic branch and substitution are in good agreement with the experimental ^{13}C NMR results. The oxygenated groups consist of ether, carbonyl and carboxyl groups, consistent with the XPS results.

Moderate deviations are observed for N and S groups between experimental and modelling results because of their low contents. The four N atoms are distributed in three amine groups and one pyridine group, while the four S atoms are involved in three sulfoxide groups and one thiophene group.

Microstructure characterization

In this section, ten Cambrian kerogen units are adopted to build the bulk kerogen model, meeting the reported minimized size requirement for 1700 atoms per unit cell (Collell et. al., 2004). As seen from the simulation box of Cambrian kerogen model (Figure 4a), the kerogen structure is highly disordered and no remarkable stacking of aromatic clusters can be observed. This is because that Cambrian kerogen has a small size of polyaromatic clusters (1 or 2 benzene rings) which are connected by bendable aliphatic branches and heteroatom groups, causing the folding of aromatic units. Figure 4b presents the pore distribution of Cambrian kerogen model. These helium probed pores in the kerogen system are mainly isolated, and are observed to be poorly connected.

Properties of Cambrian kerogen model were further computed as shown in Table 5. The simulated physical density is 1.22 g/cm^3, which is in the range of experimental data (1.18-1.25 g/cm^3) for high mature type II kerogen (Okiongbo et. al., 2005). The helium-probed porosity of Cambrian kerogen model is 21.10 %, fairly close to the reported organic matter porosities (4.45-22.50 %) in Barnett mudstone (Loucks et. al., 2009). The consistency of density and porosity between simulated and experimental results further validate our Cambrian kerogen model. The porosities and specific surface areas probed by helium are much smaller than these of innate porous structures with a probe diameter of zero. This means that ultra-micropore is the dominant pore type in the kerogen model. These ultra-micropores cannot be accessed by gaseous molecules, which cause the storage and transport limit. Small differences of innate porous properties between externally accessible regions and total regions are observed, indicating that these are only a few dead pores in the system. The pore volume and specific surface area distributions of Cambrian kerogen model are compared in Figure 5. Pore size distribution of the kerogen model shows a monopeak type, with the pore width corresponding to the peak site at ~1.6 Å. Most of the pore volumes and specific surface areas are contributed by the ultra-micropores with pore width ranging between 1 and 3 Å.

Conclusions

In this work, we generate a representative molecular model of Cambrian kerogen based on analytical data. The kerogen skeleton is composed of small aromatic clusters (1-2 benzene rings) connected by short aliphatic chains ($(CH_2)_n$, $n<4$) and heteroatom groups. The aromatic carbons are highly substituted (δ=0.53), while the aliphatic carbons are highly branched (BI=0.53). Ether groups, amine groups and sulfoxide groups are the dominant heteroatom groups for O, N and S, respectively. The kerogen model shows a reasonable representation of the realistic Cambrian kerogen in terms of structural parameters, generic compositions, physical density and porosity. The sterical kerogen structure is highly disordered and shows a remarkable folding of aromatic units. Externally accessible ultra-micropore is the dominant pore type in the Cambrian kerogen system, while the pores accessible for gas molecules are poorly connected. This generated kerogen model can serve as a starting point to study gas adsorption and transport mechanism in nanoporous network of Cambrian kerogen at nanoscale.

Acknowledgments

This work was supported by the National Natural Science Foundation of China (Grant No. 51774298 and 51504265) and the Science Foundation for the Excellent Youth Scholars of China University of Petroleum (Beijing) (Grant No.2462015YQ0223). Computer time for this study was provided by the HP High Performance Computing Cluster of the State Key Laboratory of Heavy Oil Processing at China University of Petroleum (Beijing).

References Cited

Collell, J., P. Ungerer, G. Galliero, M. Yiannourakou, F. Montel, and M. Pujol, 2014, Molecular simulation of bulk organic matter in Type II shales in the middle of the oil formation window: Energy Fuels, v. 28/12, p. 7457-7466.

Connolly, M.L., 1983, Solvent-accessible surfaces of proteins and nucleic acids: Science, v. 221/4612, p. 709-713.

Curtis, J.B., 2002, Fractured shale-gas systems: AAPG Bulletin, v. 86/11, p. 1921-1938.

Huang, L., Z.F. Ning, Q. Wang, R.R. Qi, J. Li, Y. Zeng, et al., 2017a, Thermodynamic and structural characterization of bulk organic matter in Chinese Silurian Shale: Experimental and molecular modeling studies: Energy Fuels, v. 31/5, p. 4851-4865.

Huang, L., Z.F. Ning, Q. Wang, H.T. Ye, and H.B. Qin, 2017b, Molecular Simulation of CO_2 sequestration and enhanced gas recovery in gas rich shale: An insight based on realistic kerogen model: SPE Abu Dhabi International Petroleum Exhibition & Conference held in Abu Dhabi, UAE, 13-16 November 2017, SPE-188216.

Huang, L., Z.F. Ning, Q. Wang, W.T. Zhang, Z.L. Cheng, X.J. Wu, et al., 2018a, Effect of organic type and moisture on CO_2/CH_4 competitive adsorption in kerogen with implications for CO_2 sequestration and enhanced CH4 recovery: Appl. Energy, v. 210, p. 28–43.

Huang, L., Z.F. Ning, Q. Wang, R.R. Qi, Y. Zeng, H.B. Qin, et al., 2018b, Molecular simulation of adsorption behaviors of methane, carbon dioxide and their mixtures on kerogen: Effect of kerogen maturity and moisture content: Fuel, v. 211, p. 159-172.

Kelemen, S.R., M. Afeworki, M.L. Gorbaty, M. Sansone, P.J. Kwiatek, C.C. Walters, H. Freund, M. Siskin, A.E. Bence, D.J. Curry, M. Solum, R.J. Pugmire, M Vandenbroucke, M. Leblond, and F. Behar, 2007, Direct characterization of kerogen by X-ray and solid-state 13C nuclear magnetic resonance methods: Energy Fuels, v. 21/3, 1548-1561.

Loucks, R.G., R.M. Reed, S.C. Ruppel, and D.M. Jarvie, 2009, Morphology, genesis and distribution of nanometer-scale pores in siliceous mudstones of the Mississippian Barnett Shale: J. Sediment. Res., v. 79/12, p. 848-861.

Okiongbo, K.S., A.C. Aplin, and S.R. Larter, 2005, Changes in type II kerogen density as a function of maturity: Evidence from the Kimmeridge clay formation: Energy Fuels, v. 19/6, p. 2495−2499.

Wu, K.L., Z.X. Chen, X.F. Li, X.H. Dong, 2016, Methane storage in nanoporous material at supercritical temperature over a wide range of pressures: SCI REP-UK 6, 33461.

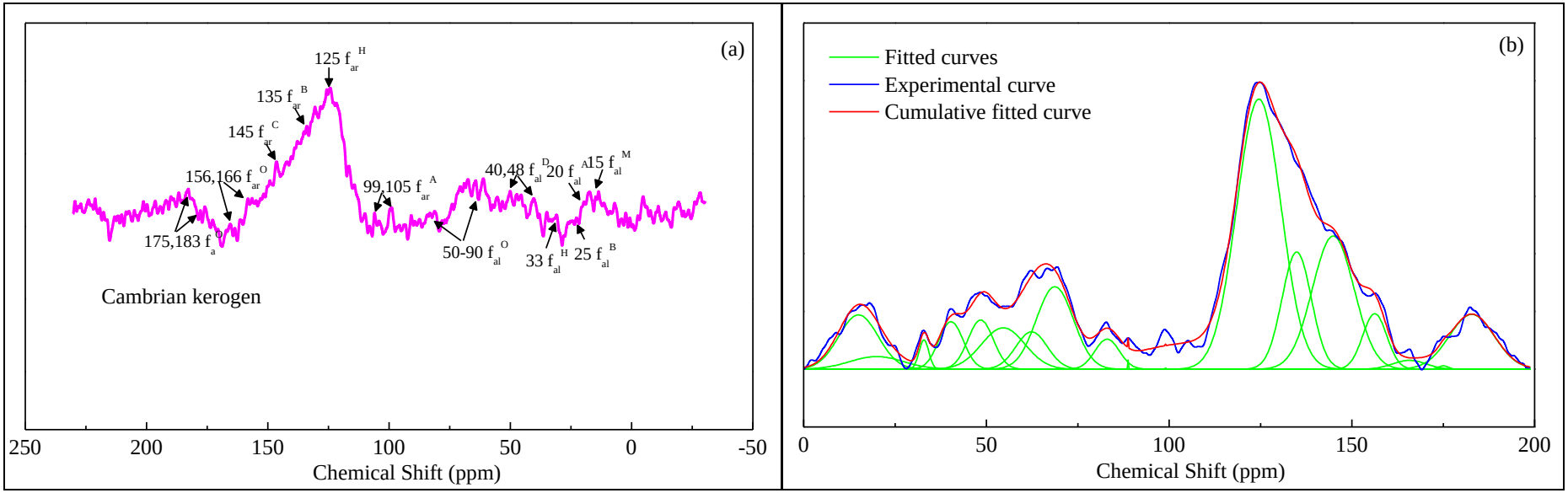

Figure 1. ^{13}C NMR spectrum of Cambrian kerogen. (a) Experimental spectrum; (b) fitting spectrum.

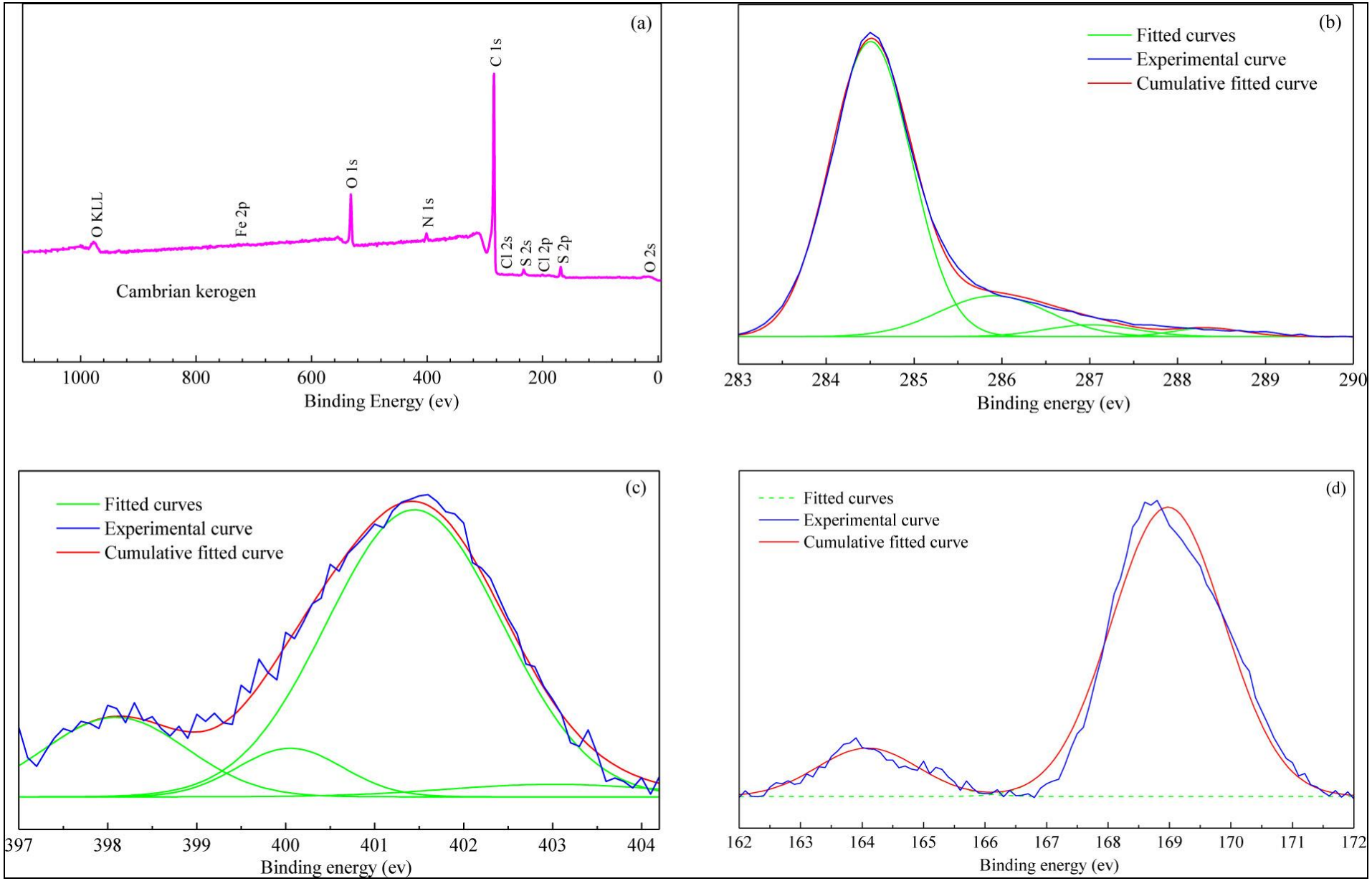

Figure 2. XPS spectra of Cambrian kerogen. (a) Experimental spectrum; (b) fitting spectra of C 1s signal; (c) fitting spectra of N 1s signal; (d) fitting spectra of S 2p signal.

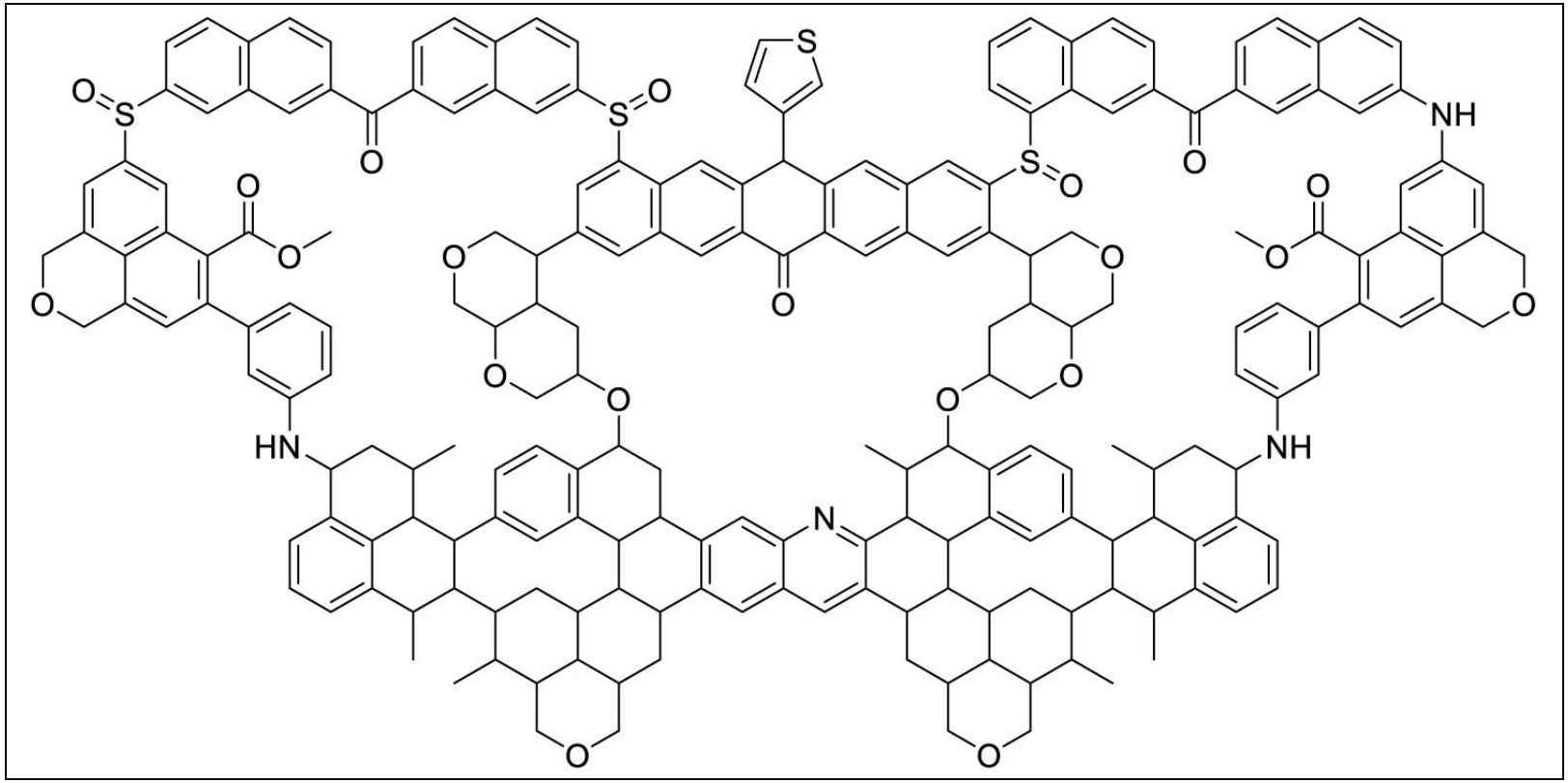

Figure 3. Molecular structure of Cambrian kerogen ($C_{210}H_{184}O_{20}N_4S_4$).

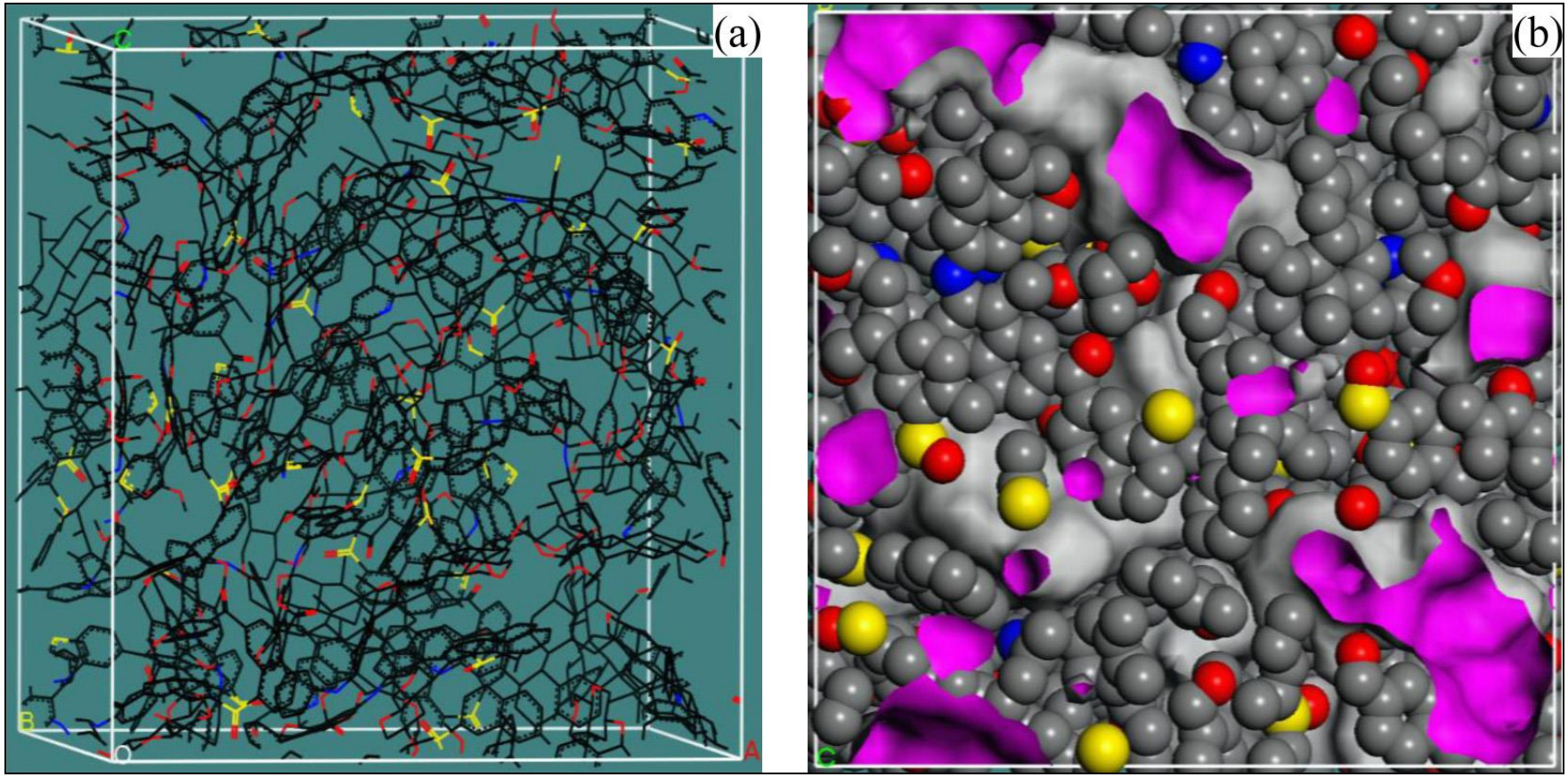

Figure 4. (a) Simulation box of Cambrian kerogen model. Atom representation: black for carbon, red for oxygen, blue for nitrogen, yellow for sulfur. (b) Pore distribution of Cambrian kerogen model probed by He. Skeleton atoms are wrapped by the purple pore surfaces.

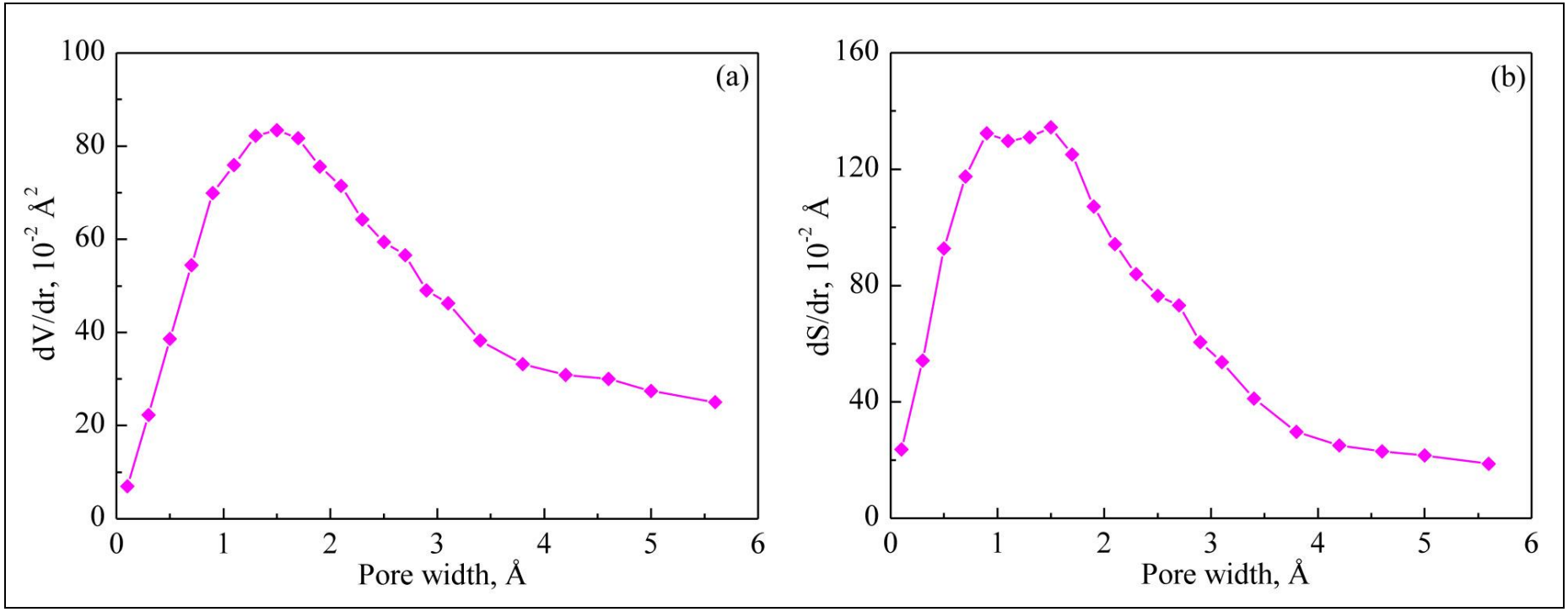

Figure 5. Pore structure of Cambrian kerogen model. (a) Pore volume distribution. (b) Specific surface area distribution.

Structural parameter	Chemical shift (ppm)	Carbon type	Location	Area fraction (%)
f_{al}^{M}	15	Aliphatic methyl	C_{al}-C*H_3	5.29

Table 1. Carbon structural parameters from ^{13}C NMR spectrum of Cambrian kerogen.

Element	Functional group	Binding energy (eV)	Peak area ratio (%)
C 1s	C-C, C-H	284.51	79.70
	C-O, C-OH	285.98	11. 79
	C=O	287.05	3.13
	COOH, COOR	288.45	2.37
N 1s	Pyridine	398.09	15.80
	Pyrrole	400.05	7.46
	Amine	401.45	73.38
	NO_x	403.01	3.35
S 2p	Sulfoether	162.13	0.00
	Pyrite	163.10	0.00
	Thiophene	164.09	13.57
	Sulfoxide	168.97	86.43

Table 2. Lattice parameters derived from ^{13}C NMR spectrum of Cambrian kerogen.

Element	Functional group	Binding energy (eV)	Peak area ratio (%)
C 1s	C-C, C-H	284.51	79.70
	C-O, C-OH	285.98	11. 79
	C=O	287.05	3.13
	COOH, COOR	288.45	2.37
N 1s	Pyridine	398.09	15.80
	Pyrrole	400.05	7.46
	Amine	401.45	73.38
	NO_x	403.01	3.35
S 2p	Sulfoether	162.13	0.00
	Pyrite	163.10	0.00
	Thiophene	164.09	13.57
	Sulfoxide	168.97	86.43

Table 3. Elementary forms for heteroatom in Cambrian kerogen derived from XPS spectrum.

Property	Structural parameter	Experimental	Modelling
Atomic compositions	H/C	0.87	0.88
	O/C	0.093	0.095
	N/C	0.019	0.019
	S/C	0.018	0.019
C groups	f_{al}	30.87 %	36.19 %
	f_{ar}	62.95 %	61.43 %
	C_n	0.07	0.18
	X_{BP}	0.16	0.16
	BI	0.53	0.53
	δ	0.53	0.50
O groups	Carbonyl (mol % C~O)	15.89	17.64
	Ether (mol % C~O)	59.99	58.82
	Carboxyl (mol % C~O)	24.12	23.53
N groups	Pyridine (mol % N)	15.80	25.00
	Pyrrole (mol % N)	7.46	0.00
	Amine (mol % N)	73.38	75.00
	NO_x	3.35	0.00
S groups	Sulfoether (mol % organic S)	0.00	0.00
	Thiophene (mol % organic S)	13.57	25.00
	Sulfoxide (mol % organic S)	86.43	75.00

[a] Experimental atomic compositions are derived from elemental analysis. Experimental C groups are derived from ^{13}C NMR spectrum. Experimental O, N and S groups are derived from XPS spectrum.

Table 4. Compositional and structural parameters of Cambrian kerogen[a]

Structure	Density (g/cm^3)	Porosity (%)			Specific surface area (m^2/g)		
		He	VDW[b]	VDW[c]	He	VDW[b]	VDW[c]
Kerogen	1.22	21.10	40.04	40.20	1637	4207	4229 6

[a] Probe diameter of He molecule is 2.6 Å. VDW[b] refers to a probe diameter of zero defined over the externally accessible regions, while VDW[c] is equivalent to a probe diameter of zero defined over the whole pore regions.

Table 5. Properties of Cambrian kerogen model at 300 K and 1 bar[a]